

## Evolution of a coastal upwelling event during summer 2004 in the southern Taiwan Strait

ZHANG Caiyun<sup>1\*</sup>, HONG Huasheng<sup>1</sup>, HU Chuanmin<sup>2</sup>, SHANG Shaoling<sup>1</sup>

<sup>1</sup> State Key Laboratory for Marine Environmental Science, College of Oceanography and Environmental Sciences, Xiamen University, Xiamen 361005, China

<sup>2</sup> College of Marine Science, University of South Florida, St. Petersburg, USA

Received 18 January 2010; accepted 27 September 2010

©The Chinese Society of Oceanography and Springer-Verlag Berlin Heidelberg 2011

### Abstract

A coastal upwelling event in the southern Taiwan Strait (STWS) was investigated using intensive cruise surveys (four repeated transects in a month) and satellite data in July and early August 2004. The extensive upwelling-associated surface cold water was first observed in early July ( $\sim 2.0 \times 10^4$  km<sup>2</sup>) along the STWS coast. Then, the cold surface water reduced in size by  $\sim 50\%$  with decreased chlorophyll concentrations after 15 days, indicating the weakening of the upwelling event. At the end of July, the cold surface water disappeared. The temporal variations of the surface cold water and the 3-D hydrography around Dongshan Island are thought to be mainly attributed to the weakened upwelling-favorable southwestern wind, the asymmetric spatial structure of the wind field and the intrusion of warm water from the northern South China Sea.

**Key words:** coastal upwelling, evolution, SST, ocean color, remote sensing, Taiwan Strait

### 1 Introduction

Upwelling is an important process in the ocean, by which deep, cold, nutrient-rich water is brought to the surface, stimulating new production and phytoplankton biomass. However, there is great variability in the coastal upwelling processes, mainly related to changes in wind strength and direction (Brink, 1983; Mann and Lazier, 1996; Chavez et al., 2002; Ramp et al., 2005). For example, within the 6-month season of upwelling off Oregon, there are four or five periods of strong upwelling separated by periods of little or no upwelling (Mann and Lazier, 1996).

The Taiwan Strait (TWS) is located between the South China Sea (SCS) and the East China Sea (ECS) (Fig.1). During summer, southwest monsoon prevails. Following the wind pattern, the horizontal advection in the TWS mainly originates from the SCS, normally referred to as Yuedong coastal water and/or South China Sea shelf water. Meanwhile, such a wind pattern is favorable for inducing coastal upwelling along the mainland coast (see review by Hu et al., 2003; Shang et al., 2004; Tang et al., 2002; Gan et al., 2009). The coastal upwelling in the southern TWS has been investigated since the 70's (Chen et al., 1982; Hong, et al., 1991; Xiao et al., 1988). It occurs in the shal-

low channel ( $\sim 40$  m average water depth) between the Taiwan Bank and the East Guangdong-South Fujian coast, which has a complicated dynamic and frontal structure (Li et al., 2000; Wang et al., 2001) and thus becomes one of the main summer fishing grounds in China Sea. Furthermore, this upwelling was suggested to contain two sub-systems, Yuedong and Minnan upwelling, separated in the vicinity of Dongshan Island with different temporal patterns within the three-month season of upwelling (June to August) (Li and

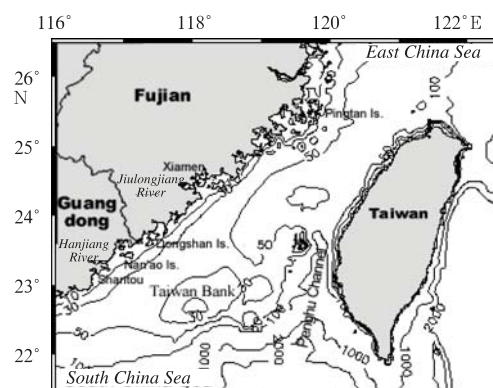


**Fig.1.** Map of the Taiwan Strait, overlaid with the bathymetry contours in meters.

Foundation item: The China's National Science Foundation grants 40331004, 40706041, 90711005 and 40521003.

\*Corresponding author, E-mail: cyzhang@xmu.edu.cn

Li, 1989). There have also been limited reports (e.g., Hong et al., 1991) that the upwelling center might be shifted between the vicinity of Dongshan Island and offshore Shantou from June to August. However, the details of the short-term transitions have never been reported in the literature.

In this paper, based on intensive in situ surveys and synoptic satellite mapping, we document the short-term evolution of a coastal upwelling event in this region from 6 July to 2 August in 2004.

## 2 Data sources

In situ data were collected along four cruise transects in the southern TWS from 6 to 23 July 2004 and from 26 July to 2 August 2004, respectively (Figs 2 and 3). These data include surface temperature, salinity, and chlorophyll fluorescence measured using a SeaBird SBE21 thermosalinographer and a WETLabs WETStar fluorometer. The flow-through in vivo fluo-

rescence was calibrated to chlorophyll-a concentration (Chl,  $\text{mg m}^{-3}$ ) using water samples from the discrete stations (Zhang et al., 2006). In addition, CTD data were collected using a SeaBird SBE 19 CTD profiler during the last two transects. Sample locations are shown in Fig. 2.

Daily MODIS (Moderate Resolution Imaging Spectroradiometer)/Aqua Level-2 sea surface temperature (SST,  $^{\circ}\text{C}$ ) and Chl data were obtained from the US NASA Goddard Space Flight Center (GSFC), and then mapped to a cylindrical equidistant projection at  $\sim 1$  km/pixel resolution. MODIS Chl data over  $<30$  m waters were excluded due to satellite algorithm artifacts (Zhang et al., 2006). Daily wind field from QuikSCAT were obtained from the US NASA PODAAC. Daily wind vectors of the first 5 pixels close to the mainland coast on each scan line were averaged. Three-day mean latitudinal distribution of wind vectors were thus produced by averaging the daily wind vectors for each three-day period.

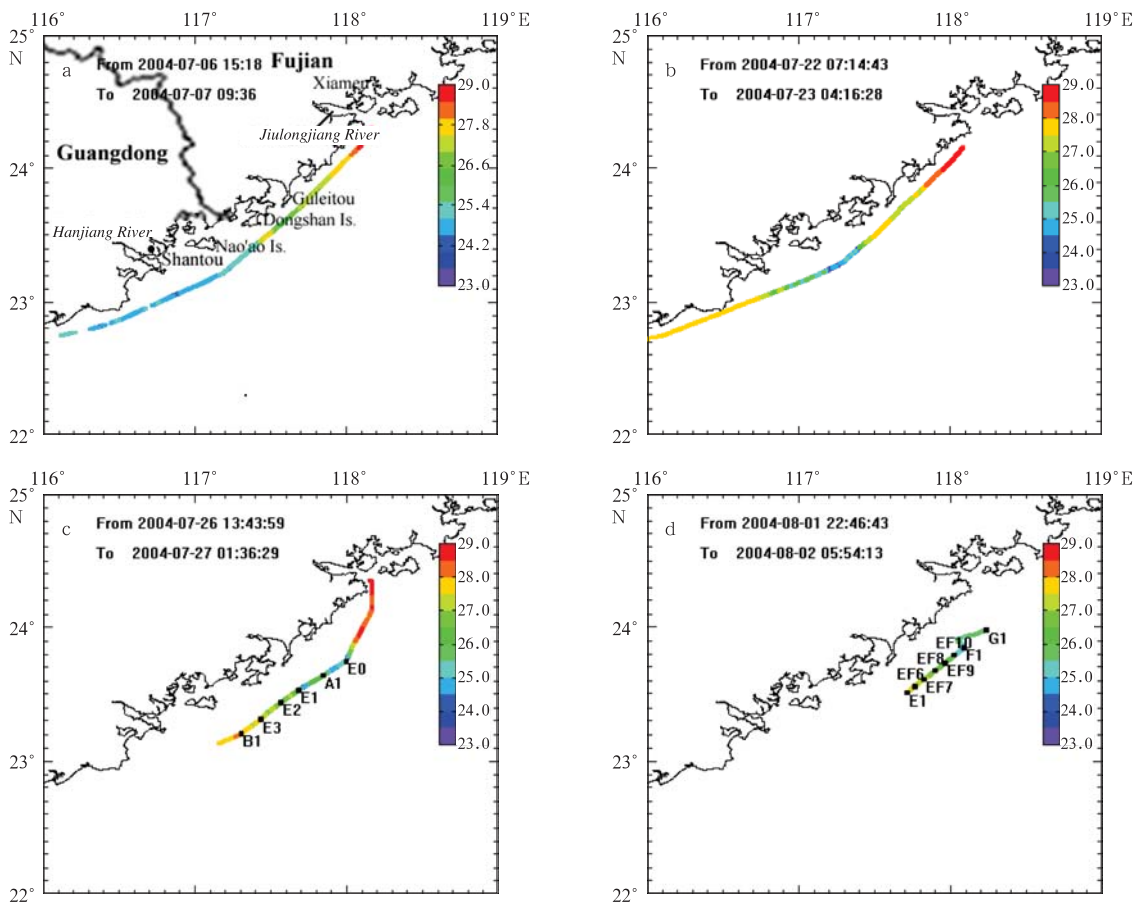


**Fig.2.** Surface temperature along the cruise transects during July and August 2004, overlaid with CTD stations.

### 3 Results and discussion

Figures 2 and 3 show the surface temperature, salinity, and Chl along the four cruise transects. During 6 to 7 July, a distinct cold belt with surface temperature  $<26\text{ }^{\circ}\text{C}$  and salinity  $\sim 34.4$  was observed along the eastern Guangdong and southern Fujian coast, where upwelling has been most frequently observed (Li and Li, 1989; Hong et al., 1991; Hu et al., 2003). The cold belt extended northward to  $23.45^{\circ}\text{N}$  where it encountered a strong front that might be influenced by the Hangjiang River plume (Fig. 3a). SST increased by about  $2\text{ }^{\circ}\text{C}$  and surface salinity decreased by 0.6 across the front. By 22–23 July, the length of the surface cold water (temperature  $<26\text{ }^{\circ}\text{C}$  and salinity  $>34.2$ ) decreased to about 40 km (Figs 2b and 3b) and was limited to between  $\sim 23^{\circ}\text{N}$  and  $23.45^{\circ}\text{N}$ . South and north of this zone, the upper layer was occupied by warm ( $\sim 28\text{ }^{\circ}\text{C}$ ) and less saline ( $\sim 33.6$ ) water. By

26–27 July, cold surface water (SST  $<26\text{ }^{\circ}\text{C}$ ) was found north of Dongshan Island ( $\sim 23.75^{\circ}\text{N}$ ), and by 1–2 August it slightly shifted to the north around  $23.86^{\circ}\text{N}$ .

MODIS SST images provided more synoptic view of the surface cold patches (Fig. 4). Because of the RMS difference of  $1.39\text{ }^{\circ}\text{C}$  between in situ and MODIS SST in the Taiwan Strait and cloud contamination on MODIS SST, a threshold of  $28\text{ }^{\circ}\text{C}$  was chosen to delineate cold from warm waters (white outlines in Fig. 4). On 29 June, no surface cold patch occurred off the southwestern coast. Later on 11 July, a large area ( $\sim 2.0 \times 10^4\text{ km}^2$ ) of cold water ( $<28\text{ }^{\circ}\text{C}$ ) appeared, covering the region both north and south of Dongshan Island. On 24 July, the size of the surface cold water north of Dongshan Island reduced to  $\sim 8.8 \times 10^3\text{ km}^2$  (Fig. 4c). Due to cloud contamination, it was difficult to judge if there was any cold patches south of Dongshan Island solely based on MODIS SST data. One week later and on 31 July, while surface cold water appeared to have shifted further north to cover most of the Zone B, south of Dongshan Island (Fig. 4d) the cold water was replaced by surface warm water. Consequently, over the 20-day period from 11 July to 31 July, the average SST of Zone A (south of Dongshan Island, outlined on Fig. 4a) in the southwestern TWS increased from  $\sim 28.1\text{ }^{\circ}\text{C}$  ( $n=12\ 309$ ) to  $\sim 30.0\text{ }^{\circ}\text{C}$  ( $n=12\ 298$ ). In addition, a tongue of warm water ( $>28\text{ }^{\circ}\text{C}$ ) associated with Jiulongjiang River plume was distinct in Zone B, stretching northeastward. Whether it is forced by the upwelling coastal jet, as the Pearl River plume observed over the northern South China Sea shelf (Gan et al., 2009), is beyond the scope of this study.

By integrating the in situ underway mapping and remote sensing observations, we suggest that a coastal upwelling event occurred in the southern TWS during 6 to 11 July, and had reduced its size and intensity during 22 to 24 July. During July 26 to 2 August, the event further weakened or even ceased in the south of Dongshan Island, but the surface cold patch maintained in the north of Dongshan Island with its position shifting northward and offshore.

Consistent with the surface signatures, vertical structures of salinity, temperature and Chl on the two transects also showed a tendency of northward shift of low temperature, high salinity, and high Chl waters during 26 July to 2 August (Fig. 5). During 26 to 27 July, the entire upper 1–8 m layer was dominated by waters of temperature  $<25\text{ }^{\circ}\text{C}$  between Sta.

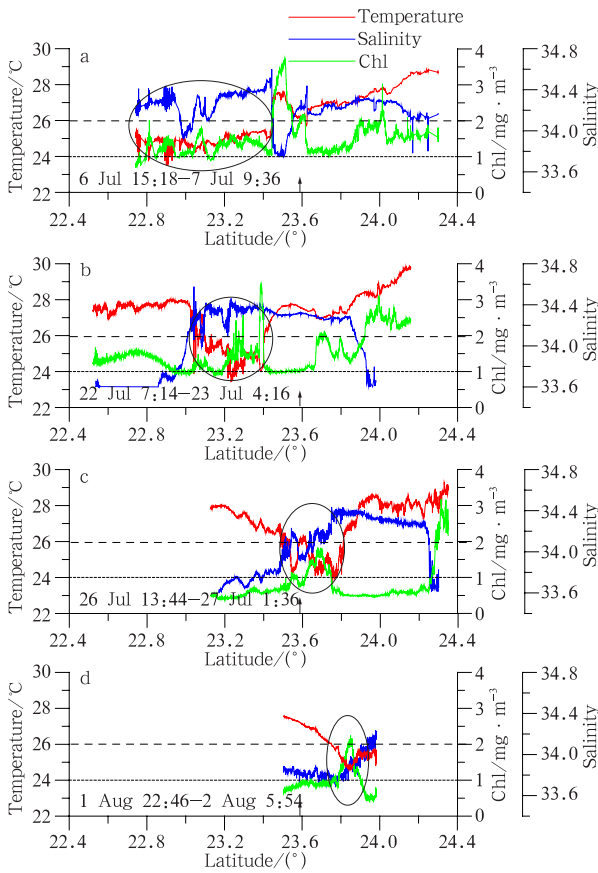


**Fig.3.** Surface temperature, salinity, and Chl along the four cruise transects (locations shown in Fig. 2). The dashed lines denote  $26\text{ }^{\circ}\text{C}$ . The dot lines denote Chl of  $1.0\text{ mg}\cdot\text{m}^{-3}$ . The arrows denote the southern tip of Dongshan Island.

A1-E0. The thermocline uplifted sharply to  $\sim 3$  m at Sta. E0. Later, during August 1 to 2 low temperature ( $< 25$  °C) and high salinity ( $> 34.3$ ) water was missing

at Sta. E0, but shifted  $\sim 20$  km northward to Sta. F1-G1. The thermocline was deepened with the vertical temperature gradient decreased.

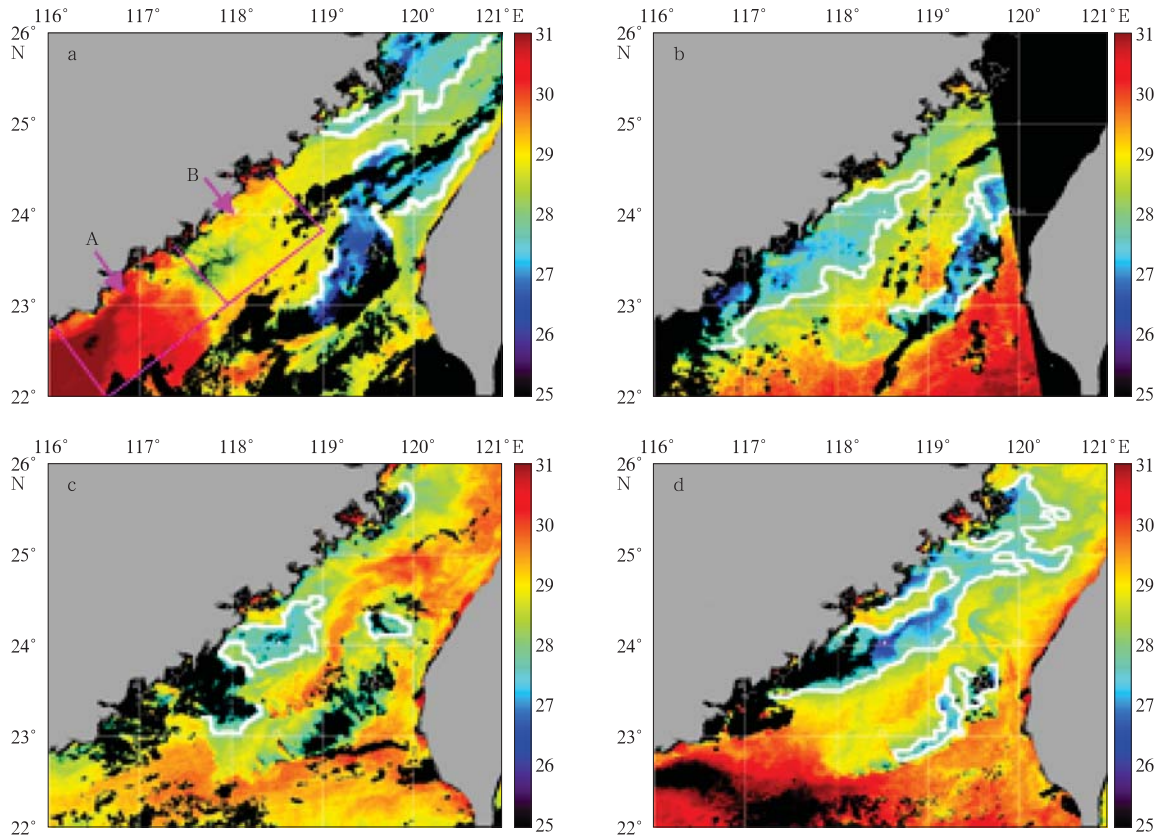


**Fig.4.** MODIS sea surface temperature (SST) images on 29 June (a), 11 July (b), 24 July (c) and 31 July (d) 2004. The 28 °C isotherm is outlined in white.

In response to the upwelling event, high Chl anomaly was observed (Figs 3 and 5). During 6 to 7 and 22 to 23 July, surface Chl in the cold water was  $> 1.0$   $\text{mg}\cdot\text{m}^{-3}$ , while higher concentration ( $> 2.0$   $\text{mg}\cdot\text{m}^{-3}$ ) was found near the upwelling/plume front (Figs. 3a and 3b). Then, on 26 to 27 July, Chl decreased to  $< 1.0$   $\text{mg}\cdot\text{m}^{-3}$  for most of the ship transects, especially south of Dongshan Island where the cold surface water had disappeared (Fig. 3c). Only one narrow band ( $< 20$  km) of high surface Chl was found around 23.7°N. Vertical profiles of Chl showed similar features where a high Chl front was found between Sta. A1 and E0 (23.6–23.72°N) (Fig. 5c). On 1 to 2 August, a narrow high Chl band appeared further to the north at 23.85°N, co-located with the cold water (Fig. 3d); and the Chl was high through the entire water column around Sta. F1 (Fig. 5f). As a consequence of the weakened or ceased upwelling event south of Dongshan Island, the average MODIS Chl for

Zone A (south of Dongshan Island, see Fig. 4a for the location) decreased from 0.49  $\text{mg}\cdot\text{m}^{-3}$  on 11 July to 0.34  $\text{mg}\cdot\text{m}^{-3}$  on 25 July, while average Chl for Zone B (north of Dongshan Island, see Fig. 4a for the location) remained unchanged.

These observed variations from 6 July to 2 August may be related to the temporal changes of the upwelling favorable wind. The southwesterly wind prevailed in early July as revealed by QuikSCAT (Fig. 6), which would lead to the offshore Ekman transport (Brink, 1983) and therefore induce extensive and cold surface water ( $\sim 2.0 \times 10^4$   $\text{km}^2$ ) on 11 July, leading to subsequent high phytoplankton biomass in the southwestern TWS. During mid July and early August, the wind became weak and variable in direction. On 15 and 26 to 27 July, two cyclones passing by the northern SCS (images not shown) produced a spatially asymmetric wind pattern in the TWS (Fig. 6). This, combined with the advection of warm water

from the northern SCS (Figs 4d and 5a), may have greatly weakened the surface transport and upwelling,

which in turn led to increased SST and decreased Chl. Nevertheless, other processes such as tidal mixing

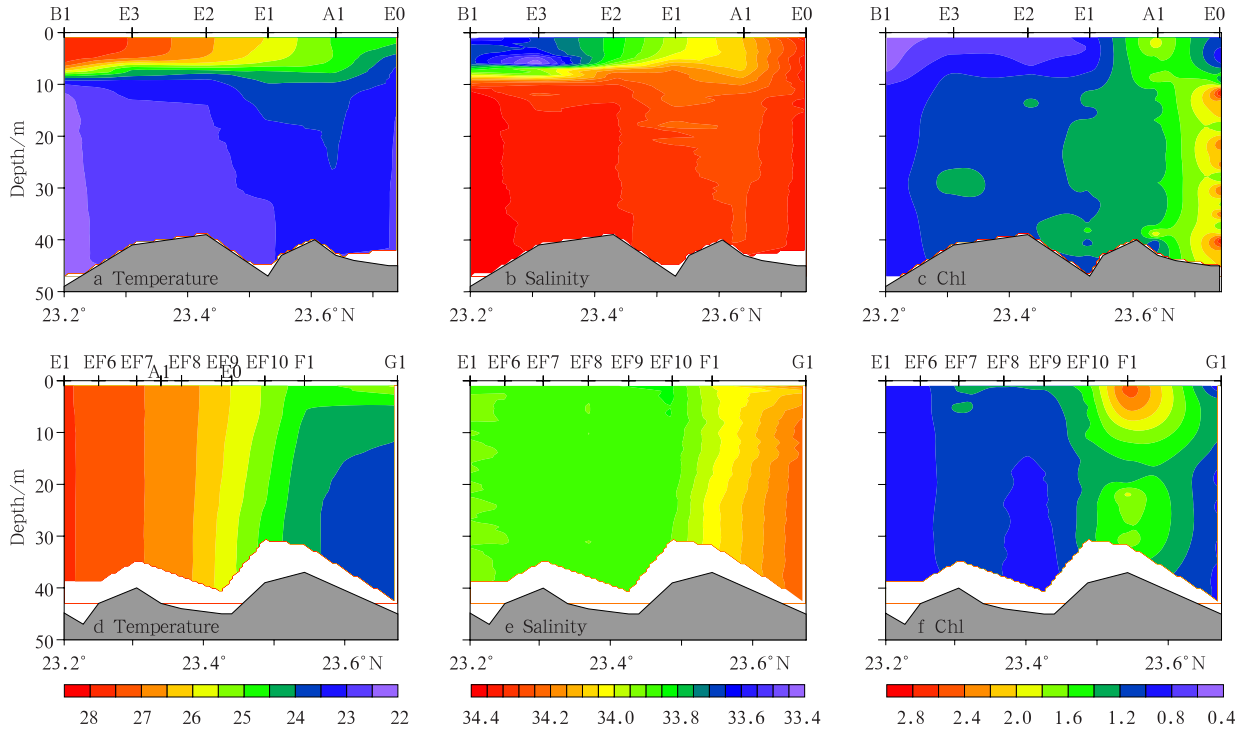


**Fig.5.** Vertical distributions of temperature, salinity and WetStar Chl along the southwestern TWS coast on 26–27 July (upper panel) and 1–2 August 2004 (lower panel).

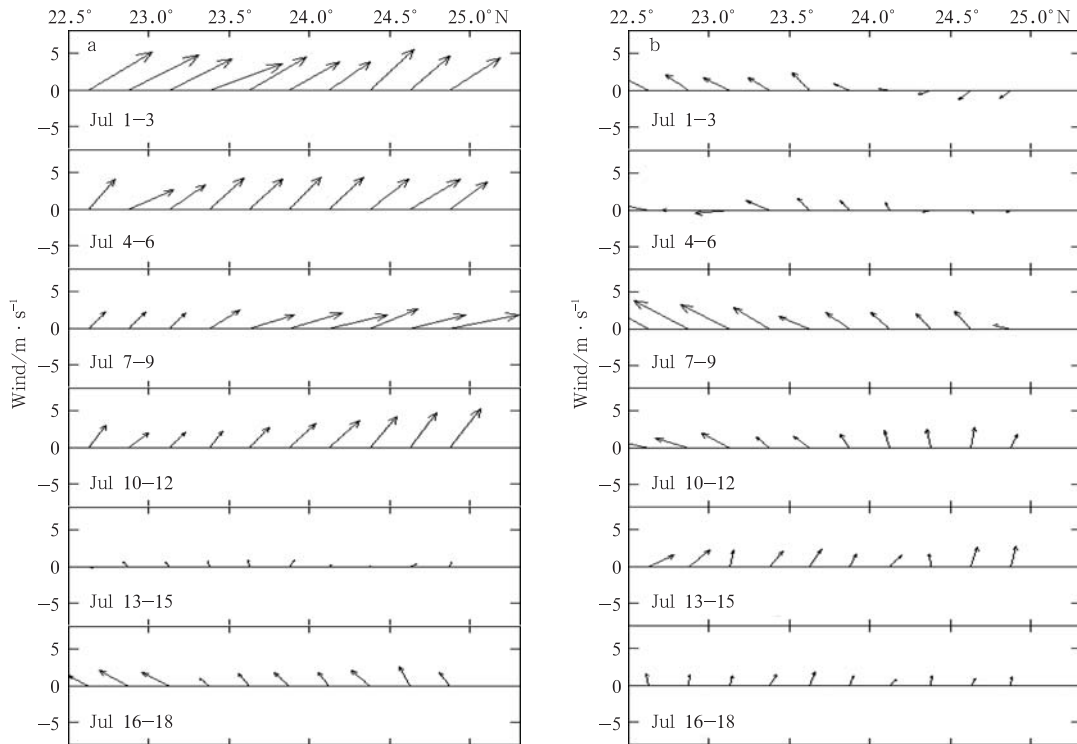


**Fig.6.** Latitudinal variation of wind vector for 3-day composite during 1 July and 5 August in the southern TWS.

and river plume may couple together with the upwelling, leading to the observed patterns. An interdisciplinary investigation with buoy, ADCP and numerical modeling will be required to improve our understanding of the upwelling processes in this complex region.

#### 4 Conclusions

For a long time the initiation and evolution of coastal upwelling events in the TWS have remained largely a mystery. Here, short-term evolution of a coastal upwelling event in the southern TWS was studied using intensive cruise surveys (four repeated transects in a month) and satellite data in July and early August 2004. Strong coastal upwelling occurred along the southwestern TWS coast in early July, which induced extensive cold surface water ( $\sim 2.0 \times 10^4 \text{ km}^2$ ) with high Chl concentrations. Then, the cold water reduced by  $\sim 50\%$  in size with decreased Chl, indicating the weakening of the upwelling by early August. Although the exact mechanism for such variations needs to be further investigated with inter-disciplinary studies (e.g., current measurement and numerical modeling), according to the 3-D hydrography and satellite data we believe that the weakened upwelling-favorable wind, the asymmetric spatial structure of the wind field and the intrusion of warm water from the northern SCS might explain this phenomenon to some extent. The detailed time-series of synoptic satellite and 3D field observations helped reveal the dynamic structure of the upwelling that has not been documented before. Such observations will further our knowledge in understanding the cause, initiation, variation, and consequence of upwelling events in this region.

#### Acknowledgments

We thank the NASA SeaWiFS and MODIS project team for providing satellite data. The QuikSCAT wind data were obtained from the Physical Oceanography Distributed Active Archive Center (PO.DAAC) at the NASA Jet Propulsion Laboratory, Pasadena, CA.

#### References

- Brink K H. 1983. The near-surface dynamics of coastal upwelling. *Progress oceanography*, 12: 223–257
- Chavez F P, J T Pennington, C G Castro, et al. 2002. Biological and chemical consequences of the 1997-98 El Nino in central California waters. *Progress in Oceanography*, 54: 205–232
- Chen J Q, Fu Z L, Li F X. 1982. A study on upwelling in Minnan-Taiwan Shoal Fishing Ground (in Chinese). *Journal of Oceanography in Taiwan Strait*, 1(2): 5–13
- Gan J, Cheung A, Guo X, et al. 2009. Intensified upwelling over a widened shelf in the northeastern South China Sea. *Journal of Geophysical Research*, 114, C09019, doi:10.1029/2007JC004660
- Hong H S, Qiu S Y, Ruan W Q, et al. 1991. Minnan-Taiwan Bank fishing ground upwelling system study, In *Minnan-Taiwan Bank Fishing Ground Upwelling Ecosystem Study*, Hong H S, et al. (eds). Beijing: Science Press, 1–10
- Hu J, Kawamura H, Hong H. 2003. A review of research on the upwelling in the Taiwan Strait. *Bulletin of Marine Science*, 73(3): 605–628
- Li L, Li D. 1989. Summer hydrographic features of channel west of Taiwan shoals and the coastal upwelling. *Journal of Oceanography in Taiwan Strait(in Chinese)*, 8(4): 353–359
- Li L, Guo X G, Wu R. 2000. Oceanic fronts in southern Taiwan Strait. *Journal of Oceanography in Taiwan Strait (in Chinese)*, 19(2): 147–156
- Mann K H, J R N Lazier. 1996. *Dynamics of marine ecosystem: Biological-physical interactions in the oceans*. Oxford: Blackwell Publishing
- Ramp S R, J D Paduan, I Shulman, et al. 2005. Observations of upwelling and relaxation events in the northern Monterey Bay during August 2000. *J Geophys Res*, 110, C07013, doi:10.1029/2004JC002538
- Shang S L, Zhang C Y, Hong H S, et al. 2004. Short-term variability of chlorophyll associated with upwelling events in the Taiwan Strait during the southwest monsoon of 1998. *Deep Sea Research*, 51(10-11): 1113–1127
- Tang D L, Kester D R, Ni I, et al. 2002. Upwelling in the Taiwan Strait during the summer monsoon detected by satellite and shipboard measurements. *Remote sensing of environment*, 83: 457–571
- Torres R, Barton E D, Miller P, et al. 2003. Spatial patterns of wind and sea surface temperature in the Galician upwelling system. *Journal of Geophysical Research*, 108(C4), 3130, doi: 10.1029/2002JC001361
- Wang D X, Liu Y, Qi Y Q, et al. 2001. Seasonal variability of thermal fronts in the northern South China Sea from satellite data. *Geophys Res Lett*, 28: 3963–3966
- Xiao H. 1988. Studies of coastal upwelling in western Taiwan Strait. *Journal of oceanography in Taiwan Strait(in Chinese)*, 7(2): 135–142
- Zhang C, Hu C, Shang S, et al. 2006. Bridging between SeaWiFS and MODIS for continuity of chlorophyll-a concentration assessments off southeastern China. *Remote Sensing of Environment*, 102: 250–263